

Interactive comment on “In situ interactive characteristics of reactive minerals in soil colloids and soil carbon preservation differentially revealed by nanoscale secondary ion mass spectrometry and X-ray absorption fine structure spectroscopy”

Jian Xiao et al.

yuguanghui@njau.edu.cn

Received and published: 26 May 2016

Associate Editor Decision: Publish subject to minor revisions (Editor review) (26 May 2016) by Dr. Roland Bol

Comments to the Author:

Figure 1 exist of 12 sub figures, in the text it is not clear what specific sub figures is referred too when all 3 treatments have a, b, c and d. One should use individual letter for each sub figure.

The authors may want to considering putting some of these 12 sub figures into supplementary material and only show the key sub figures.

The authors should in the revised version implement all what is promised in response to the posed comments in the interactive discussion and a final check of the English be useful.

Response to Associate Editor

Comment1: Figure 1 exist of 12 sub figures, in the text it is not clear what specific sub figures is referred too when all 3 treatments have a, b, c and d. One should use individual letter for each sub figure.

The authors may want to considering putting some of these 12 sub figures into supplementary material and only show the key sub figures.

Response 1: Many thanks for the above-mentioned suggestions from the Associate Editor. In the revised manuscript, we only presented the results of high-resolution transmission electron microscopy (HRTEM) images of colloids extracted from the NPKM fertilized soil. And the HRTEM images of the control- and NPK- fertilized soils have been put into supplementary materials as Fig. S2, and the two sets of “a, b, c and d” have been changed to “a, b, c, d for the sub-figures under Control and e, f, g and h for the sub-figures under NPK” in the new Fig. S2, accordingly.

Comment 2: The authors should in the revised version implement all what is promised in response to the posed comments in the interactive discussion and a final check of the English be useful.

Response 2: In the revised manuscript, we have implemented all valuable comments into the manuscript and carefully checked the English writings. The implemented comments and the revised areas have been presented in red color in the revised manuscript.

Marked Manuscript Version

New strategies for submicron characterization the carbon binding of reactive minerals in long-term contrasting fertilized soils: Implications for soil carbon storage

Jian Xiao^{1,7,8}, Xinhua He^{2,3}, Jialong Hao^{3,4}, Ying Zhou^{4,5}, Lirong Zheng^{4,5,6}, Wei Ran¹, Qirong Shen¹, Guanghui Yu^{1,6,7,*}

¹ National Engineering Research Center for Organic-based Fertilizers, Jiangsu Collaborative Innovation Center for Solid Organic Waste Resource Utilization, Jiangsu Provincial Key Lab for Organic Solid Waste Utilization, Nanjing Agricultural University, Nanjing 210095, China.

² [Centre of Excellence for Soil Biology, College of Resources and Environment, Southwest University, Chongqing 400715, China.](#)

³ School of Plant Biology, University of Western Australia, Crawley, WA 6009, Australia.

³⁻⁴ Key Laboratory of Earth and Planetary Physics, Institute of Geology and Geophysics, Chinese Academy of Science, Beijing 100029, China.

^{4,5} Shanghai Institute of Measurement and Testing Technology, Shanghai 201203, China.

⁵⁻⁶ Beijing Synchrotron Radiation Facility, Institute of High Energy Physics, Chinese Academy of Sciences, Beijing 100049, China.

^{6,7} Department of Plant Pathology, North Carolina State University, Raleigh, NC 27695, USA.

⁷⁻⁸ Department of Earth and Environmental Engineering, Columbia University, New York, NY 10027, USA.

* Correspondence to: G. H. Yu (yuguanghui@njau.edu.cn or gyu6@ncsu.edu)

Abstract. Mineral binding is a major mechanism for soil carbon (C) stabilization. However, the submicron information about the *in situ* mechanisms of different fertilization practices affecting organo-mineral complexes and associated C preservation remains unclear. Here, we applied nano-scale secondary ion mass spectrometry (NanoSIMS), X-ray photoelectron spectroscopy (XPS), and X-ray absorption fine structure spectroscopy (XAFS) to examine differentiating effects of inorganic versus organic fertilization on interactions between highly reactive minerals and soil C preservation. To examine such interactions, soils and their extracted colloids were collected during a 24-year long-term fertilization period (1990-2014) (no-fertilization, Control; chemical nitrogen (N), phosphorus (P) and potassium (K) fertilization, NPK; and NPK plus swine manure fertilization, NPKM). The results for different fertilization conditions showed a ranked soil organic matter (SOM) concentration with NPKM > NPK > Control. Meanwhile, oxalate extracted Al (Al_o), Fe (Fe_o), short range ordered (SRO) Al (Al_{xps}), Fe (Fe_{xps}), and dissolved organic carbon (DOC) ranked with NPKM > Control > NPK, but the ratios of DOC/Al_{xps} and DOC/Fe_{xps} ranked with NPKM > NPK > Control. Compared with the NPK treatment, the NPKM treatment enhanced the C binding loadings of Al and Fe minerals in soil colloids at the submicron scale. Furthermore, a greater concentration of highly reactive Al and Fe minerals was presented under NPKM than under NPK. Together, these submicron scale findings suggest that both the reactive mineral species and their associations with C are differentially affected by 24-year long-term inorganic and organic fertilization.

Key words: Al and Fe minerals; carbon binding capability; inorganic and organic fertilization; nano-scale secondary ion mass spectrometry (NanoSIMS); organo-mineral complexes; X-ray absorption

fine structure spectroscopy (XAFS); reactive minerals; carbon binding capability; X-ray photoelectron spectroscopy (XPS)

1. Introduction

45 Associations of organic matter (OM) with pedogenic minerals, which are termed as organo-mineral complexes, are known to be key controls in the biogeochemical processes that retain OM in natural soil system (Torn et al., 1997; Kögel-knbaner et al., 2008; Mikutta et al., 2009; Schmidt et al., 2011). Soil OM (SOM) preferentially binds to rough surfaces, which provide a multitude of reactive mineral surfaces (Chen et al., 2014; Vogel et al., 2014). These reactive minerals are also termed as short-range
50 ordered (SRO) meta-stable colloidal minerals in volcanic ejecta (Torn et al., 1997), and serve as the nuclei for soil organic carbon (SOC) storage (Hochella et al., 2008; Kögel-Knabner et al., 2008; Remusat et al., 2012; Vogel et al., 2014). Therefore, these reactive Al and Fe minerals including Al and Fe minerals in soil play a critical role in determining C stability (Solomon et al., 2012; Hernes et al., 2013).

55 On the other hand, the reactive mineral surface of organo-mineral complexes in the complex soil matrix (mainly the top-soil layer) could be greatly improved through organic amendments to soil, such as the anthropogenic importation of organic fertilizers under long-term experimentation (Schmidt et al., 2011; Hernandez et al., 2012; Yu et al., 2012; Wen et al., 2014a; Abdala et al., 2015). Based on a meta-analysis of 49 sites and 130 observations in the world, Maillard and Angers (2014) found that
60 cumulative manure input had a dominant effect on SOC stock changes when compared to no fertilization and chemical fertilization (Maillard and Angers, 2014). Furthermore, it was estimated that cumulative manure-C input resulted in a relative SOC change factor of 1.26 ± 0.14 (95% Confidence Interval (CI)). Another meta-analysis by compiling a data set of 83 studies assessed and identified the

65 effects of improved farming practices on SOC sequestration in China ~~by compiling a data set of 83~~
~~studies~~ (Zhao et al., 2015), and indicating that SOC concentration and stocks at 0-30 cm depth were
significantly increased under organic fertilization ~~when compared to~~ than under no fertilization and
chemical fertilization. Although our previous results had shown that manure amendments enhanced
reactive components of minerals (i.e., ferrihydrite and allophane) in soils by selective extraction
methods, spectroscopies and high resolution-transmission electron microscopy (HRTEM) observation
70 (Yu et al., 2012; Wen et al., 2014a and 2014b; Huang et al., 2016), little is known about the impacts of
different fertilization practices on the *in situ* associations between reactive minerals and SOC in soil
colloids at submicron scale.

In general, *in situ* investigations of natural organo-mineral complexes are restricted to bulk analyses
of operationally defined physical fractions (Hatton et al., 2012 and 2015; Remusat et al., 2012; Vogel et
75 al., 2014). In contrast, techniques for direct visualization at the submicron scale could greatly aid in
gaining a better understanding of the interactions between organic structures and reactive minerals
(Remusat et al., 2012; Vogel et al., 2014; Xiao et al., 2015). For instance, nano-scale secondary ion
mass spectrometry (NanoSIMS) has the potential to examine the spatial integrity of soil
microenvironments and has been designed for high lateral resolution (down to 50 nm) imaging, while
80 still maintaining high mass resolution and high sensitivity (mg kg⁻¹ range) (Herrmann et al., 2007; Xiao
et al., 2015). Previous studies have shown that NanoSIMS is an effective technique for studying natural
organo-mineral complexes at the submicron scale (Herrmann, 2007; Mueller et al., 2012; Remusat et al.,
2012; Hatton et al., 2012 and 2015; Vogel et al., 2014). However, NanoSIMS can not determine the

morphology, elemental composition and mineral species. High-resolution transmission electron
85 microscopy (HRTEM) combined with selected area electron diffraction (SAED) is also a promising
technique that can determine the morphology and provide detailed information on organo-mineral
surfaces, as well as changes in their surface chemistries (Wen et al., 2014a; Yaron-Marcovich et al.,
2005). Although direct observations of organo-mineral complexes by NanoSIMS and HRTEM have
been previously described (Ramos et al., 2013; Vogel et al., 2014; Rumpel et al., 2015), few studies
90 have reported the effects of fertilization practices on the organo-mineral complexes in soil colloids. In
addition, X-ray photoelectron spectroscopy (XPS) can identify the oxidation state of elements on the
surface (2~10 nm) of minerals (Zhu et al., 2014). Compared with XPS technique, X-ray absorption fine
structure spectroscopy (XAFS) is a powerful tool for both identification and quantification of different
mineral phases presenting in soil colloids (Li et al., 2015; Xiao et al., 2015).

95 Using soil colloids extracted from 24-year fertilized soils (1990-2014), the objective of this study
were to address 1) the effects of fertilization practices on the quantity and composition of Al and Fe
minerals, and 2) the *in-situ* interactions between SOC and minerals at the submicron scale.

2. Materials and methods

2.1. Soil samples

100 Samples of soil (Ferralic Cambisol, FAO soil taxonomic classification) were from a long-term
(1990-2014) fertilization site in Qiyang, Hunan, Southern China (26°45'N, 111°52'E, 120 m above sea
level). The long-term fertilization experiment, which belongs to the Institute of Agricultural Resources
and Regional Planning, Chinese Academy of Agricultural Sciences, has been under an annual rotation

of wheat and corn cropping system since September 1990. The topsoil contained 61.4% clay, 34.9% silt
105 and 3.7% sand. Three fertilization treatments with 2 replicates or plots (20 m × 10 m) for each treatment
were examined as follows: 1) no fertilization (Control), 2) chemical nitrogen (N), phosphorus (P) and
potassium (K) (NPK) and 3) a combination of the chemical fertilizers with swine manure (NPKM) (see
Fig. S1 for detailed fertilization rates). The NPK and MNPK had the same total application of 300 kg N
ha⁻¹ yr⁻¹. The applied N was 100% urea in the NPK, but was 30% from urea with the remaining 70%
110 from swine manure in the MNPK. A 1.0-m-deep cement buffer zone was constructed between each plot.
Each soil sample was a composite of twenty random cores (5 cm internal diameter auger) collected at
0-20 cm depth from one replicate plot. The fresh soil was mixed thoroughly, air-dried, and sieved (5
mm) for further analyses.

2.2. Soil colloids extraction and quantitation of highly reactive Al and Fe minerals

115 The soil colloids extraction was based on a previously described method (Schumacher et al., 2005).
Briefly, 100 g of fresh soils was suspended in 500 mL of deionized water on a horizontal shaker (170
rpm) for 8 hr at 25 ± 1°C, and centrifuged at 2500 g for 6 min (Fig. S1). Aliquots of the supernatant
suspensions and freeze-dried soil colloid samples were then generated. Quantitation of highly reactive
minerals, including Al and Fe minerals (Al_o, Fe_o), was performed using the acid ammonium-oxalate
120 extraction method (Kramer et al., 2012). In brief, soil was extracted using 0.275 M ammonium oxalate
at pH 3.25 with a ~~1:100~~ soil :_extractant = 1 : 100 (w/v) ratio. Ammonium oxalate was used to
selectively remove short-range ordered hydrous oxides of Fe and Al such as ferrihydrite and allophane.

2.3. HRTEM analysis

HRTEM samples were prepared by dropping soil mobile colloids onto carbon coated copper grids.

125 The images were recorded at an acceleration voltage of 200 keV using a JEOL JEM-2100F microscope (JEOL JEM-2100F, Japan), which was at the Analysis and Testing Centre of Nanjing Normal University, China. HRTEM images, selected area electron diffraction (SAED) and energy dispersive X-ray analysis (EDX) were conducted using the JEOL JEM-2100F microscope to characterize soil colloid samples.

130 **2.4. NanoSIMS analyses**

For NanoSIMS measurements, several aliquots of the colloidal suspension from these three different fertilization treatments were separately dropped onto a silicon wafer and air-dried. In this study, we achieved 6 NanoSIMS images for each soil colloid sample to support the replicates of our results (Philippe and Schaumann, 2014; Xiao et al., 2015). For every sample, all 6 spots were analyzed to
135 obtain a reliable data basis for the calculation of the fate of $^{12}\text{C}^-$, $^{27}\text{Al}^{16}\text{O}^-$, and $^{56}\text{Fe}^{16}\text{O}^-$ (Table S2).

The analyses were performed on a NanoSIMS 50L (Cameca, Gennevilliers, France) instrument at the Institute of Geology and Geophysics, Chinese Academy of Sciences, [Beijing](#), China. Prior to analysis, the gold coating layer (30 nm) and any possible contamination of the sample surface were sputtered using a high primary beam current (pre-sputtering). During the pre-sputtering, the reactive Cs^+
140 ions were implanted into the sample to enhance the secondary ion yields. The primary beam (~ 0.9 pA) focused at a lateral resolution of 100-200 nm, was scanned over the samples, and the secondary ion images of $^{12}\text{C}^-$, $^{27}\text{Al}^{16}\text{O}^-$, and $^{56}\text{Fe}^{16}\text{O}^-$ were simultaneously collected by electron multipliers with an electronic dead time fixed at 44 ns. The presence of $^{12}\text{C}^-$ ion mass indicated SOC, while the presence of

$^{27}\text{Al}^{16}\text{O}^-$ and $^{56}\text{Fe}^{16}\text{O}^-$ demonstrated Al and Fe minerals, respectively. We compensated for the charging
145 due to the non-conductive mineral particles using the electron flood gun of the NanoSIMS instrument.
All measurements were conducted in an imaging mode. The dwell time was 1 ms pixel⁻¹ for all
acquisitions. In this study, the NanoSIMS images sizes were 256 × 256 pixels, Control, no fertilization,
28 × 28 μm²; NPK, chemical nitrogen, phosphorus and potassium fertilization, 30 × 30 μm²; NPKM,
chemical NPK plus swine manure fertilization, 25 × 25 μm², respectively. Specific and relevant details
150 describing NanoSIMS measurements can be found in previous publications (Vogel et al., 2014; Rumpel
et al., 2015; Xiao et al., 2015). ~~Other specific details describing NanoSIMS measurements can be found
in previous publications (Vogel et al., 2014; Xiao et al., 2015).~~

The analyses were carried out on different cluster compositions using the Image J software with the
OpenMIMS plugin (http://www.nrimshms.harvard.edu/NRIMS_ImageJ.php). In this study, regions of
155 interest (ROIs) were selected according to the intensity of the secondary $^{12}\text{C}^-$ ion mass. After
pre-sputtering, since all measurements on the NanoSIMS instruments were done in an image mode, the
pixels on the images from the lowest to the highest could show the intensity of the secondary $^{12}\text{C}^-$ ion
mass and also represent the real distribution and heterogeneity of soil MOAs (Herrmann et al., 2007;
Mueller et al., 2012; Rumpel et al., 2015; Vogel et al., 2014). In this study, the visible SOC surface areas
160 were divided into rich and less rich $^{12}\text{C}^-$ ROIs according to the pixel value extracted from the
NanoSIMS images. The $^{12}\text{C}^-$ rich ROIs included the areas above 90 pixels and the $^{12}\text{C}^-$ less rich ROIs
included the areas in the range of 90-40 pixels under Control and NPK, while the $^{12}\text{C}^-$ rich ROIs were
above 50 pixels and the $^{12}\text{C}^-$ less rich ROIs were in the range of 50-30 pixels under NPKM. The

threshold option of the Image J software was used to automatically generate the ROIs from these
165 NanoSIMS images. In doing so, the triangle algorithm was used (Vogel et al., 2014; Xiao et al., 2015).
The same ROIs were simultaneously selected in the $^{27}\text{Al}^{16}\text{O}^-$ and $^{56}\text{Fe}^{16}\text{O}^-$ images.

2.5. XPS analyses

The sample preparation for the XPS procedures was adapted from Gerin et al. (2003). The XPS
data were collected using a PHI 5000 Versa Probe X-ray photoelectron spectrometer (UIVAC-PHI,
170 Japan) equipped with a monochromatized Al K α X-ray source (1486.69 eV). The binding energy scale
was corrected using the adventitious hydrocarbon C 1s spectrum (C 1s = 284.6 eV) (Zhu et al., 2014).
The analyzed zone corresponded to a 300 $\mu\text{m} \times 300 \mu\text{m}$ elliptical spot. The surface charge induced by
the photo ejection process was balanced using a flood gun at 6 eV. To optimize the signal to noise ratio,
spectra were recorded at a detector resolution corresponding to 0.125 eV per channel. The base pressure
175 in the spectrometer was 6.7×10^{-10} Torr. The XPS data analyses were performed using XPSPEAK 4.1
with Shirley background correction, as referenced at <http://www.lasurface.com/xps/index> and
<http://srdata.nist.gov/xps/Default.aspx>. No fixed full width at half maximum (FWHM) values were
determined for the spectra of soil colloids collected under contrasting fertilization treatments.
Gaussian-Lorentzian ratios were freely fit for all peaks in this study (Liang et al., 2008).

180 2.6. XAFS spectra analyses

Fe K-edge X-ray absorption fine structure (XANES) and extended X-ray absorption fine structure
(EXAFS) spectra were recorded at the beamline 1W1B at the XAFS Station of the Beijing Synchrotron
Radiation Facility (BSRF, Beijing, China) using a Si (111) double-crystal monochromator. The storage

ring was operated at 2.5 GeV with the electron current decreasing from 240 to 160 mA within
185 approximately 8 hrs. Samples were ground into fine powders and brushed onto tapes, which were then
stacked together to yield approximately one X-ray-absorption length at their corresponding metal edges.
The intensities of incident and transmitted X-rays were monitored by ionization chambers filled with
nitrogen gas. All reported spectra were measured at 20°C. Spectra were collected in quick-scan and
transmission mode. XANES spectra were recorded with 0.5 eV step, counting 10 s from 7,100 to 7,800
190 eV. EXAFS spectra were recorded up to $k = 14.0 \text{ \AA}^{-1}$, using 1 eV steps and counting for 100–200 s per
scan. To improve data quality, 5 XANES scans and 5 EXAFS scans were recorded for each sample. The
X-ray energy scale was calibrated to the iron K-edge (7112.0 eV) using an iron metal foil prior to XAFS
acquisition. Averaged spectra were normalized using Athena (Version 2.1.1, California, USA) software,
and EXAFS data were extracted using the Autoback routine, using the same program. The spectra were
195 normalized by subtracting a first-order polynomial fitted to the data from –100 to –30 eV before the
edge and subsequently dividing through a second-order polynomial fitted to the data from 60 to 450 eV
above the edge. Linear combination fitting (LCF) of XANES data were performed with the respective
functions of Athena. EXAFS spectra were extracted using the Autobk algorithm (Rbkg = 0.9; k-weight
=3, spline k-range 0–11.8 \AA^{-1}). The Fe K-edge XANES spectra with LCF of eight standard iron samples
200 were used to precisely characterize the composition of Fe minerals (Baumgartner et al., 2013; Senn et
al., 2015). The standard iron samples (either purchased or synthesized) of ferrous sulfate, ferrous
oxalate, ferric sulfate, ferric oxalate, goethite, hematite, ferrihydrite, and maghemite were also recorded
in a transmission mode, ~~which were purchased or synthesized~~ (Table S3). A standard was considered to

have a substantial contribution if it accounted for more than 10% of a linear combination fit. The quality
205 of the LCF was given by the residual value, the goodness-of-fit parameter R , defined by $R =$
 $6[I_{\text{exp}}(E) - I_{\text{cal}}(E)]^2 / 6[I_{\text{exp}}(E)]^2 \times 100$ where I_{exp} and I_{cal} are the absorption of the experimental and
calculated spectra, respectively.

2.7. Chemical analyses

The concentration of SOC was quantified using a CN analyzer (Vario EL, Elementar GmbH, Hanau,
210 Germany), while SOM was $1.724 \times \text{SOC}$. Soil pH was determined using a pH electrode at a 1:5 soil:
distilled water ratio. The concentration of Fe and Al was quantified by inductively coupled plasma
atomic emission spectroscopy (710/715 ICP-AES, Agilent, Australia). The concentration of DOC was
determined by a TOC/TN analyzer (multi N/C 3000, Analytik Jena AG, Germany).

2.8. Statistical analyses

215 One-way analysis of variance (ANOVA) was used to test the effects of long-term fertilization on
~~reactive iron minerals~~ physiochemical characteristics in the soil. Significant differences between
treatments (means \pm SE, $n = 3$) were determined by Tukey's HSD post hoc test at $P < 0.05$, where the
conditions of normality and homogeneity of variance were met.

3. Results

220 3.1. Concentration and morphology of organo-mineral complexes in soil colloids under contrasting fertilizations

Compared with a soil pH of 5.47 under Control, ~~the~~ soil pH significantly ($P < 0.05$) decreased to
4.15 under NPK but significantly ($P < 0.05$) increased to 5.84 under NPKM (Table 1). SOM

concentrations ~~in~~ under different fertilization ~~treatments~~ ranked as NPKM > NPK > Control (Table 1).
225 A general higher of the Oxalate-oxalate extracted Al (Al_o), Fe (Fe_o), SRO Al (Al_{xps}), Fe (Fe_{xps}), and
DOC ranked as NPKM > Control > NPK, but ~~ratios of the~~ DOC/ Al_{xps} and DOC/ Fe_{xps} ratios ranked as
NPKM > NPK > Control (Table 1).

To get insight into the spatial distribution of SOM associated with reactive mineral particles, we
used both HRTEM and NanoSIMS to acquire *in situ* observations of such associations. At the
230 nanometer scale, the HRTEM images of extracted soil colloids provided direct visualization of the
presence of soil SRO minerals from Control-, NPK- and NPKM-fertilized soil samples (Fig. 1 and Fig.
S2). Soil minerals showed amorphous and crystalline patterning in different regions (Fig. 1-a, b and
Figs. S2-a, b, e, f). The SAED (selected area electron diffraction) pattern further demonstrated that the
amorphous mineral species were dominated by Al, Si, and O, while the crystalline minerals were mainly
235 composed of Fe and O (Fig. 1-c, d and Figs. S2-c, d, g, h).

The NanoSIMS images of $^{12}C^-$, $^{27}Al^{16}O^-$, and $^{56}Fe^{16}O^-$ ion masses showed the submicron elemental
distribution and spatial heterogeneity in the soil colloids (Figs. 2 and Fig. S32). The color bar on the
NanoSIMS images, from blue to white directly showed the ion masses intensity from the relatively
weak to strong at a spatial and submicron scale. Under different fertilizations, the characterization of
240 organo-mineral complexes were randomly distributed and highly heterogeneous. Meanwhile, the
arrangement and intensity were obviously various among the $^{12}C^-$, $^{27}Al^{16}O^-$, and $^{56}Fe^{16}O^-$ ion masses.

3.2. Binding capability of C by Al and Fe minerals

We next used the region of interests (ROIs) to explore the C binding capability of Al and Fe

minerals. Fig. S32 presents a representative NanoSIMS image, which is able to showing the position of
245 region of interests (ROIs) among the several replicates (spots) of different fertilization treatments
(Control: 8 replicates; NPK: 6 replicates; NPKM: 6 replicates, respectively). Based on the pixel value of
secondary $^{12}\text{C}^-$ ion mass in all spots from different fertilization treatments, the selected ROIs were
identified. The selected ROIs were further divided into $^{12}\text{C}^-$ rich- and $^{12}\text{C}^-$ less rich- ROIs (Fig. S32).
Table S2 lists the quantification of $^{12}\text{C}^-$ rich ($^{12}\text{C}^-$ -R) and $^{12}\text{C}^-$ less-rich ($^{12}\text{C}^-$ -LR) ROIs. The area
250 percentage of the $^{12}\text{C}^-$ rich- or $^{12}\text{C}^-$ less rich- ROIs accounted for 7.47% or 40.18 %, 10.80% or 27.64 %
and 8.23% or 37.99% under Control, NPK and NPKM, respectively (Table S2). The area of percentage
~~for-between~~ the Control and the NPKM was similar but different from the NPK, suggesting that
compared to no fertilization control, chemical fertilization ~~er~~ can ~~could~~ change organo-mineral
associations at the submicron scale in soil colloids, but chemical plus organic fertilization (NPKM) ~~can~~
255 could eliminate the effect of chemical fertilization on organo-mineral associations. Interestingly, the
box plots (Fig. 3) of $^{12}\text{C}^-/^{27}\text{Al}^{16}\text{O}^-$ (a, b) and $^{12}\text{C}^-/^{56}\text{Fe}^{16}\text{O}^-$ (c, d) ratios showed that both the median and
the mean value were higher under NPKM than those under NPK. These results provided *in-situ*
observation evidence at the submicron scale demonstrating that more organic C had been bound by Al
and Fe minerals under NPKM than under NPK (Figs. 2 and 3), which is consistent with previous results
260 from bulk analysis-analyses (Maillard and Angers, 2014).

3.3. Chemical speciation of reactive minerals and C

The XPS Al $2p_{3/2}$ peak-fitting results (Table 2 and Fig. 4) showed that 45% allophane (~ 73.80 eV),
29.4% of boehmite (~ 74.5 eV) and 26% Al Ox (~ 75.40 eV) were present in soil colloids under NPKM.

In contrast, approximately 43% and 34% of allophane were observed in soil colloids under NPK and Control, respectively. Considering higher (over 5 times) total Al concentrations in soil colloids under NPKM than under NPK (Table 1), the amount of allophane in soil colloids ~~under NPKM is would~~ approximately be 5 times higher under NPKM than ~~that of~~under NPK.

Linear combination fitting (LCF) of soil colloids (Fig. S43 and Table 3) showed that goethite (56.8%-67.0%) and hematite (14.9%-25.0%) were prominent under all three fertilization treatments. The remaining Fe phases were composed of the less crystalline ferrihydrite species. The percentage of ferrihydrite was the highest under NPKM ($18.0 \pm 0.02\%$), followed by under Control ($16.0 \pm 0.03\%$) and under NPK ($6.30 \pm 0.02\%$). In view of the better C binding and potential preservation capability of ferrihydrite when compared to goethite and hematite (Baker et al., 2010; Kramer et al., 2012; Lalonde et al., 2012; Xiao et al., 2015), it ~~is was~~ reasonable to conclude that there ~~is was a~~ greater C loading by Fe minerals under organic fertilization than under chemical fertilization. ~~This~~ These results ~~is are~~ consistent with the previous meta-analysis (Maillard and Angers, 2014) ~~but while evidencing provides an in-situ observation evidence~~ at the submicron scale.

Furthermore, Fe K-edge EXAFS was used for qualitative analysis of the composition of Fe minerals in soil colloids. The Fe k^3 -weighted EXAFS spectra (Fig. 5, left) showed that the spectral features of soils colloids under Control and NPKM were more similar to those of goethite, hematite, and ferrihydrite than to other minerals or compounds, suggesting that those Fe minerals ~~are could be~~ mainly composed of goethite, hematite, and ferrihydrite. The spectral features of the soils under NPK were more similar to those of goethite and hematite than to those of other minerals or compounds, supporting

that those Fe minerals ~~are~~ could be mainly composed of goethite and hematite rather than the short-range ordered ferrihydrite. Specifically, the EXAFS of Fe oxides showed double antinodes at 9.2 and 11.6 Å⁻¹ under Control and NPKM, whereas triple antinodes were observed under NPK at 9.2, 10.3 and 11.6 Å⁻¹ (Fig. 5, left). Double antinodes were found in hematite and ferrihydrite, whereas triple antinodes were observed in goethite. These results implied that the coordination environment for Fe-Fe linkages in Control and NPKM samples might be different from that in NPK samples because the observed peak primarily derived from the Fe-Fe coordination in goethite (Mitsunobu et al., 2012).

Fourier transforms showed that Fe minerals under Control and NPKM had most of the features observed in goethite, hematite, and ferrihydrite [i.e., first peak (Fe-O) and second peak (edge-sharing Fe-Fe)] and amplitude of multiple-scattering peak at 5.2 Å. Specifically, the first shell at 1.5 Å corresponds to the Fe-O coordination, and the intensity and position were approximately identical between the Control or NPKM treated soil colloids and ferrihydrite spectra. In contrast, the second shell identified at $R + \Delta R = 2.3\text{-}3.5$ Å corresponding to the Fe-Fe coordination was smaller than that of ferrihydrite. These results indicated that Fe in the Control and NPKM treated soil colloids might have a weaker Fe-Fe linkage than that in ferrihydrite.

In addition, the XPS C 1s peak-fitting results (Table 2 and Fig. 4) demonstrated that aromatic C (Ar-C-C/Ar-C-H, ~284.6 eV) was dominant under all three fertilizations, with the highest percentage (75.86%) under NPKM, followed by NPK (62.51%) and Control (62.26%). In contrast, the percentages of other carbon groups, i.e., ether or alcohol carbon (C-O) and ketone or aldehyde carbon (C=O), were lowest under NPKM among the three contrasting fertilization treatments.

4. Discussion

4.1. Long-term organic fertilization increased the concentration of highly reactive Al and Fe minerals and their soil C binding capacity

~~Selective~~ The selective extraction method (Table 1) showed that organic fertilization increased 36.36% of highly reactive Al (Al_o) and 33.33% of highly reactive Fe minerals (Fe_o) compared with the Control treatment, but increased 63.64% of Al_o and 46.67% of Fe_o compared with the NPK treatment.

Therefore, organic fertilization facilitates the formation of highly reactive Al and Fe minerals. This is consistent with several previous investigations about chemical extraction methods. For example, Zhang et al. (2013) observed that the oxalate-extractable Fe (Fe_o) content of NPKM and M treatments was greater than that of N and NPK treatments in the 20–40 cm layer, but there was no statistical differences between the manure treatments (NPKM and M) and mineral fertilizer treatments (N and NPK) at 0–20 cm. Meanwhile, the pyrophosphate-extractable Fe (Fe_p) concentrations were less in the NPKM and M treatments than those in the N and NPK treatments at 0–20 cm. Using the citrate-bicarbonate-dithionite (CBD) extraction method, Huang et al. (2016) showed that organic fertilization treatments (NPKM and M) increased the iron freeness index (i.e., the Fe_d/Fe_t ratio) when compared to chemical fertilization treatment (NPK). In addition, Wen et al. (2014) found that compared with chemical fertilization (N and NPK), organic fertilization (NPKM and M) significantly ($P < 0.05$) increased amorphous Al and decreased exchangeable Al, while the addition of lime (N with lime and NPK with lime) significantly ($P < 0.05$) increased weakly organically bound Al and decreased exchangeable Al. By ^{27}Al nuclear magnetic resonance (NMR) and Fourier- transform infrared spectroscopy (FTIR) spectroscopy, Wen et

al. (2014b) confirmed the presence of amorphous Al as allophane and imogolite in soil colloids under
325 no fertilization and organic fertilization but not under chemical fertilization. However, the direct
potential of C preservation capacity by Al and Fe minerals under different fertilizations regimes remains
unexplored.

 In this study, the ROI analyses of NanoSIMS observation (Fig. 3) indicated that despite of highly
spatial heterogeneity of organo-mineral complexes at the submicron scale, long-term organic
330 fertilization strengthened the SOC binding and potential preservation capability of Fe minerals for both
the ^{12}C -rich- or ^{12}C -less rich- ROIs in soil colloids compared to chemical fertilization. Meanwhile,
long-term organic fertilization also strengthened the SOC binding and potential preservation capability
of Al minerals for the ^{12}C -rich- ROIs in soil colloids when compared to chemical fertilization. However,
as for the ^{12}C -less rich- ROIs in soil colloids, fertilization regimes seemed to have no influence in the
335 SOC binding with Al minerals. Additionally, colloids from the NPKM treated soil had higher ratios of
DOC/ Al_{xps} and DOC/ Fe_{xps} than those under Control and NPK (Table 1), which was compatible with the
assumption suggested by the NanoSIMS and HRTEM. These results could be derived from a long-term
continuous organic C input that might have enriched soil microbial communities and then in turn
supported an efficient formation of the concomitant organo-mineral aggregates (Wild et al., 2014;
340 Basler et al., 2015).

Moreover, it was notable that higher proportion of aromatic C (Ar-C-C/Ar-C-H) while lower
proportion of ether or alcohol carbon (C-O) or ketonic or aldehyde carbon (C=O) were observed under
NPKM than under NPK or Control, which indicated that additional aromatic functional groups might

have a priority attaching to the highly reactive Al and Fe minerals compared with other carbon groups.

345 | This result ~~is~~was also supported by C 1s near-edge X-ray fine structure (NEXAFS) spectroscopy that compared to the NPK treatment, the NPKM treatment markedly increased the percentages of both the aromatic (283.0-286.1 eV) and phenolic (286.2-287.5 eV) groups over 2.8-fold (Huang et al., 2016). Moreover, the XPS C 1s peak-fitting results (Table 2 and Fig. 4) demonstrated that the highest percentage of aromatic C (75.86%) was present under NPKM, followed by under NPK (62.51%) and under Control (62.26%). The previous investigation had shown that aromatic C in composted dairy manure accounted for approximately 30% of the total C, taking advantage of the solid-state ¹³C nuclear magnetic resonance (NMR) spectroscopy (Liang et al., 1996). And the addition of manure-based amendments increased SOC and enhanced aggregate stability (Mikha et al., 2015). But it is unclear whether manure is direct contributed to aromatic C increase or first utilized by microbes and then
355 | contributed to aromatic C increase in this study. Aromatic compounds are preferentially retained at the interface of reactive minerals and that long-term C storage by SRO minerals has occurred via the mechanism of chemical retention with dissolved aromatic acids (Kramer et al., 2012; Huang et al., 2016). These results were due to that the long-term continuous organic C input could improve the spatial arrangement within the mineral matrix (i.e., more amorphous minerals), the fine-scale redox
360 | environment (i.e., appropriate pH), microbial ecology (i.e., appropriate pH, manure) and interaction with mineral surfaces under fertile and weakly acidic conditions (Wild et al., 2014; Basler et al., 2015; Lehmann and Kleber, 2015).

4.2. Long-term organic fertilization modified the composition of highly reactive Al and Fe

minerals

365 Our results from both XPS, NanoSIMS and Fe K-edge XAFS showed that organic fertilization facilitated the formation of highly reactive Al and Fe minerals, e.g., allophane, imogolite, and ferrihydrite (Tables 2-3 and Figs. 3-5), which could further explain why long-term organic manure fertilization was able to improve the C and N binding capacity of Al and Fe minerals. The data from the TOC and ICP-AES (Table 1) also supported that soils under NPKM contained significantly higher

370 percentages of Al_o, Fe_o, SRO minerals, and SOM than those under NPK. The results from HRTEM and SAED (Fig. 1) further showed that soil colloids under NPKM were composed of large amounts of meta-stable amorphous or SRO minerals (e.g., allophane, imogolite and ferrihydrite), which could form stable organic-mineral bonds through anion and inner-sphere ligand-exchange reactions and would thus be well-suited to physically protecting geometries (Torn et al., 1997; Yu et al., 2012; Basler et al., 2015).

375 It would be an innovative method using the ratio of $^{12}\text{C}/^{27}\text{Al}^{16}\text{O}^-$ and $^{12}\text{C}/^{56}\text{Fe}^{16}\text{O}^-$ on NanoSIMS images to quantify the stronger binding ability ~~in under~~ NPKM ~~treatment~~ compared with ~~the~~ other fertilization treatments (Fig. 3). These results are consistent with previous studies using the ^{27}Al NMR spectroscopy and FTIR that long-term organic treatment released greater amounts of minerals into soil solutions than chemical fertilizers (NPK) treatment (Yu et al., 2012; Wen et al., 2014a,b; Wu et al.,

380 2014). Using the Fe K-edge XANES spectroscopy, Huang et al. (2016) also showed that reactive Fe minerals were mainly composed of less crystalline ferrihydrite in the Morganic manure-treated soil and more crystalline goethite in the NPK-treated soil. By measuring the composition of manure, Wen et al. (2014b) had shown that the reactive minerals introduced by the manures were very limited, ruling out

the possibility that fertilizers introduced reactive fractions. Furthermore, Huang et al. (2016) indicated
385 that organic fertilization increased the iron freeness index (i.e., Fe_d/Fe_t ratio) when compared to no
fertilization and chemical fertilization by citrate-bicarbonate-dithionite (CBD) extraction, suggesting a
high degree of soil weathering in organic fertilization. Therefore, we suggest that organic fertilization
treatments *in situ* enhance reactive minerals by the transformation of minerals. This ~~is~~ was supported by
a simulated study ~~from Huang et al. (2016)~~ that the addition of oxalic acid to soil colloids ~~can~~ could
390 promote the transformation from Fe(III) to ferrihydrite (Huang et al. 2016). Another previous report
also indicated that the low-molecular-weight (LMW) organic acid ~~may~~ might incorporate into the
network structure of SRO minerals, inhibiting further growth of SRO minerals (Xu et al., 2010).

In addition, previous studies ~~have shown~~ showed that the formation of highly reactive Al and Fe
minerals could greatly benefit the binding and potential preservation of SOC (Torn et al., 1997; Wen et
395 al., 2014a; Xiao et al., 2015). Especially, reactive Fe minerals ~~may~~ might be responsible for the
retention of aromatic C and O-alkyl C in soils (Huang et al., 2016). Under favorable conditions, SOC
turnover in soil ~~colloids~~ with highly reactive Al and Fe minerals could persist in tephra beds for at least
250,000 yrs (Parfitt, 2009). The aAccumulation of highly reactive Al and Fe minerals in soil ~~colloids~~
could therefore improve SOC sequestration under long-term organic manure fertilization. Furthermore,
400 soil colloids usually consist of mixtures or complexes of hydrous oxides of Fe, Al and natural organic
matter, which have important implications for deposition, aggregation, and sorption processes
(Schumacher et al., 2005; Herrmann et al., 2007; Mueller et al., 2012).

4.3. Environmental implications and technical challenges

Soils are highly complex materials that are structurally and elementally heterogeneous across a wide range of spatial and temporal scales (Herrmann et al., 2007; Mueller et al., 2012; Vogel et al., 2014). In porous media the stability, transport, and deposition of colloids, which usually consist of mixtures or complexes of hydrous oxides of Fe, Al, and natural organic matter, are strongly affected by the mobilized colloidal particles and specific surface area (Kaiser and Guggenberger, 2003; Schumacher et al., 2005). By combining HRTEM, NanoSIMS, XPS and/or XANES techniques, the present study investigated the previously unknown highly reactive mineral elements and their spatial distribution patterns under contrasting fertilizations. This strategy has the following key advantages: HRTEM, NanoSIMS images and elemental mapping with sufficient resolution are able to illustrate the specific relationship and spatial heterogeneity of organic, ~~highly reactive~~ mineral complexes under contrasting fertilizations, while the decomposition of XPS and Fe K-edge XANES peaks to definite semi-quantitative determinations shows the elemental valence states and compositions. Nevertheless, we are still faced with the challenge of how to utilize spatial information to parameterize models for handling the complex, stochastic interactions between organo-mineral complexes and their microenvironments, including a range of biogeochemical transformation influenced by different fertilization treatments at the submicron scale (Remusat et al., 2012; Abdala et al., 2015; Hatton et al., 2015). Because of the highly heterogeneous distribution of mineral elements/C-functional groups in soils, investigations on more regions in more samples is necessary to obtain solid relationships between organic C and mineral elements using the NanoSIMS *in situ* observation. Meanwhile, an inadequate sample preparation to avoid artefacts is also a challenge, which may introduce a bias in the

interpretation of NanoSIMS data and location of regions-of-interest (Herrmann et al., 2007). In addition,
425 | the complexity of iron chemistry in soils also makes the Fe XANES and EXAFS characterization a
challenge. For example, the accuracy of the LCF results is strongly affected by the correctness of the
applied set of predictor variables (Prietz et al., 2007). And EXAFS only provides average structural
information over a short-range order, therefore it fails to determine if the minerals are crystalline or
amorphous (Li et al., 2015), which is important in understanding the stabilization of organic carbon.

430 | With the enough soil samples and the improvement of sample preparation, these limitations can be well
overcome, and the combination of HRTEM, NanoSIMS, XPS and/or XANES technique strategy is
expected to receive wide applications in the fields of agricultural science, environmental science, and
ecology science.

5. Conclusions

435 | In this study, we showed that 24-year long-term (1990-2014) organic fertilization increased the
carbon binding loading and the potential preservation capacity of soil colloids at the submicron scale.
These submicron scale findings suggest that both reactive mineral species and their associations with C
are differentially affected by inorganic and organic fertilization. This may be attributed to a greater
concentration of highly reactive Al and Fe minerals presenting under NPKM than under NPK.
440 | Meanwhile, we also demonstrated that the combination of nano-scale secondary ion mass spectrometry
(NanoSIMS), high resolution-transmission electron microscopy (HRTEM), X-ray absorption fine
structure spectroscopy (XAFS), and X-ray photoelectron spectroscopy (XPS), is a promising strategy to
distinguish relationships between C preservation and minerals in natural soil colloids as well as the

potential for SOM accumulation under inorganic and organic fertilizations at the submicron scale. The
445 strategy paves the way toward in situ characterization of organo-mineral associations, which is critical
in understanding their associated SOM accumulation and soil carbon storage.

Supplementary material related to this article is available online at:
<http://www.biogeosciences.net/>

Acknowledgment. The authors thank B.R. Wang for his assistance in soil sampling in the Qiyang
450 Long-term Fertilization Station. We also thank the staffs from [the](#) 1W1B beamline at Beijing
Synchrotron Radiation Facility, for assistances ~~during~~ in data collection. This work was jointly
financially supported by National Natural Science Foundation of China (41371248 and 41371299),
Natural Science Foundation of Jiangsu Province of China (BK20131321), the Qing Lan Project, the
Innovative Research Team Development Plan of the Ministry of China (IRT1256), the 111 Project
455 (B12009), the Priority Academic Program Development (PAPD) of Jiangsu Higher Education
Institutions, and Research Project of Shanghai Municipal Bureau of Quality and Technical Supervision
([2014-02100RJ1414](#)).

References

- Abdala, D.B., da Silva, I.R., Vergutz, L., and Sparks, D.L.: Long-term manure application effects on
460 phosphorus speciation, kinetics and distribution in highly weathered agricultural soils, *Chemosphere*,
119, 504-514, 2015.
- Baker, L.L., Strawn, D.G., Vaughan, K.L., and McDaniel, P.A.: XAS study of Fe mineralogy in a
chronosequence of soil clays formed in basaltic cinders, *Clays Clay Min.*, 58, 772-782, 2010.

- Basler, A., Dippold, M., Helfrich, M., and Dyckmans J.: Microbial carbon recycling-an underestimated
465 process controlling soil carbon dynamics-Part 1: A long-term laboratory incubation experiment,
Biogeosciences, 12, 5929-5940, 2015.
- Baumgartner, J., Morin, G., Menguy, N., Perez Gonzalez, T., Widdrat, M., Cosmidis, J., and Faivre, D.:
Magnetotactic bacteria form magnetite from a phosphate-rich ferric hydroxide via nanometric ferric
(oxyhydr)oxide intermediates, Proc. Natl. Acad. Sci., 110, 14883-14888, 2013.
- 470 Chen, C.M., Dynes, J.J., Wang, J., Karunakaran, C., [and](#) Sparks, D.L.: Soft X-ray spectromicroscopy
study of mineral-organic matter associations in Pasture soil clay fractions, Environ. Sci. Technol.,
48, 6678-6686, 2014.
- Childs, C.W., Inoue, K., Seyama, H., Soma, M., Theng, B.K.G., and Yuan, G.: X-ray photoelectron
spectroscopic characterization of Silica Springs allophane, Clay Min., 32, 565-572,1997.
- 475 Crist, B.V.: Handbook of monochromatic XPS spectra, XPS International, LLC, Mountain View, USA,
2000.
- Gerin, P., Genet, M., Herbillon, A., [and](#) Delvaux, B.: Surface analysis of soil material by X-ray
photoelectron spectroscopy, Eur. J. Soil Sci., 54, 589-604, 2003.
- 480 Hatton-[P.J.](#), Remusat, L., Zeller, B., [and](#) Derrien, D. A multi-scale approach to determine accurate
elemental and isotopic ratios by nano-scale secondary ion mass spectrometry imaging, Rap. Commu.
Mass Spectro., 26, 1363-1371, 2012.
- Hatton-[P.J.](#), Castanha, C., Torn, M.S., and Bird, J.A.: Litter type control on soil C and N stabilization
dynamics in a temperate forest, Glob. Chang. Biol., 21, 1358-1367, 2015.

- 485 | Hernandez, Z., Almendros, G., Carral, P., Alvarez, A., Knicker, H., [and](#) Perez-Trujillo, J.P.: Influence
of non-crystalline minerals in the total amount, resilience and molecular composition of the organic
matter in volcanic ash soils (Tenerife Island, Spain), *Eur. J. Soil Sci.*, 63, 603-615, 2012.
- | Hernes, P.J., Kaiser, K., Dyda, R.Y., [and](#) Cerli, C.: Molecular trickery in soil organic matter: hidden
lignin, *Environ. Sci. Technol.*, 47, 9077-9085, 2013.
- Herrmann, A.M., Ritz, K., Nunan, N., Clode, P.L., Pett-Ridge, J., Kilburn, M.R., Murphy, D.V.,
490 | O'Donnell, A.G., [and](#) Stockdale, E.A.: Nano-scale secondary ion mass spectrometry-A new
analytical tool in biogeochemistry and soil ecology: A review article, *Soil Biol. Biochem.*, 39,
1835-1850, 2007.
- Hochella, M.F.Jr., Lower, S.K., Maurice, P.A., Penn, R.L., Sahai, N., Sparks, D.L., and Twining, B.S.:
Nanominerals, mineral nanoparticles, and Earth systems, *Science*, 319, 1631-1635, 2008.
- 495 | Huang, C.C., Liu, S., Li, R.Z., Sun, F.S., Zhou, Y., and Yu, G.H.: Spectroscopic evidence of the
improvement of reactive iron mineral content in red soil by long-term application of swine manure,
PLoS One, 11, e0146364, 2016.
- Kaiser, K., and Guggenberger, G.: Mineral surfaces and soil organic matter, *Eur. J. Soil Sci.*, 54,
219-236, 2003.
- 500 | Kögel-Knabner, I., Guggenberger, G., Kleber, M., Kandeler, E., Kalbitz, K., Scheu, S., Eusterhues, K.,
and Leinweber, P.: Organo-mineral associations in temperate soils: Integrating biology, mineralogy,
and organic matter chemistry, *J. Plant Nutr. Soil Sci.*, 171, 61-82, 2008.
- | Kramer, M.G., Sanderman, J., Chadwick, O.A., Chorover, J., [and](#) Vitousek, P.M.: Long-term carbon

storage through retention of dissolved aromatic acids by reactive particles in soil, *Glob. Chang. Biol.*, 18, 2594-2605, 2012.

Lalonde, K., Mucci, A., Ouellet, A., and Gelinas, Y.: Preservation of organic matter in sediments promoted by iron, *Nature*, 483, 198-200, 2012.

Lehmann, J., and Kleber M.: The contentious nature of soil organic matter, *Nature*, 528, 60-68, 2015.

Li, W., Joshi, S.R., Hou, G.J., Burdige, D.J., Sparks, D.L., and Jaisi, D.P.: Characterizing phosphorus speciation of Chesapeake Bay sediments using chemical extraction, ³¹P NMR, and X-ray absorption fine structure spectroscopy, *Environ. Sci. Technol.*, 49, 203-211, 2015.

Liang, B., Lehmann, J., Solomon, D., Sohi, S., Thies, J.E., Skjemstad, J.O., Luizao, F.J., Engelhard, M.H., Neves, E.G., and Wirrick, S.: Stability of biomass-derived black carbon in soils, *Geochim. Cosmochim. Acta*, 72, 6069-6078, 2008.

Liang, B.C., Gregorich, E.G., Schnitzer M., and Voroney R.P.: Carbon mineralization— in soils of different textures as affected by water-soluble organic carbon extracted from composted dairy manure, *Biol. Fertil. Soils*, 21, 10-16, 1996.

Maillard, E., and Angers, D. A.: Animal manure application and soil organic carbon stocks: a meta-analysis, *Glob. Chang. Biol.*, 2, 666-679, 2014.

Mikha, M. M., Hergert, G. W., Benjamin, J. G., Jabro, J. D., and Nielsen, R. A.: Long-term manure impacts on soil aggregates and aggregate-associated carbon and nitrogen, *Soil Sci. Soc. Amer. J.*, 79, 2, 626-636, 2015.

Mikutta, R., Schaumann, G.E., Gildemeister, D., Bonneville, S., Kramer, M.G., Chorover, J., Chadwick,

O.A., and Guggenberger, G.: Biogeochemistry of mineral-organic associations across a long-term mineralogical soil gradient (0.3-4100kyr), Hawaiian Islands, *Geochim. Cosmochim. Acta*, 73, 2034-2060, 2009.

Mitsunobu, S., Shiraishi, F., Makita, H., Orcutt, B.N., Kikuchi, S., Jorgensen, B.B., [and](#) Takahashi, Y.: Bacteriogenic Fe(III) (oxyhydr)oxides characterized by synchrotron microprobe coupled with spatially resolved phylogenetic analysis, *Environ. Sci. Technol.*, 46, 3304-3311, 2012.

Mueller, C.W., Kölbl, A., Hoeschen, C., Hillion, F., Heister, K., Herrmann, A.M., and Kögel-Knabner, I.: Submicron scale imaging of soil organic matter dynamics using NanoSIMS-From single particles to intact aggregates, *Org. Geochem.*, 42, 1476-1488, 2012.

Parfitt, R.L.: Allophane and imogolite: role in soil biogeochemical processes, *Clay Min.*, 44, 135-155, 2009.

Philippe, A., and Schaumann, G.E.: Interactions of dissolved organic matter with natural and engineered inorganic colloids: A review, *Environ. Sci. Technol.*, 48, 8946-8962, 2014.

Prietzl, J., Thieme, J., Eusterhues, K., and Eichert, D.: Iron speciation in soils and soil aggregates by synchrotron-based X-ray microspectroscopy (XANES, μ -XANES), *Europ. J. Soil Sci.*, 58, 1027-1041, 2007.

Ramos, M., Ferrer, D., Martinez-Soto, E., Lopez-Lippmann, H., Torres, B., Berhault, G., and Chianelli, R.R.: In-situ HRTEM study of the reactive carbide phase of Co/MoS₂ catalyst, *Ultramicroscopy*, 127, 64-69, 2013.

Remusat, L., Hatton, P.J., Nico, P.S., Zeller, B., Kleber, M., [and](#) Derrien, D.: NanoSIMS study of

organic matter associated with soil aggregates: advantages, limitations, and combination with
545 STXM, *Environ. Sci. Technol.*, 46, 3943-3949, 2012.

Rumpel, C., Baumann, K., Remusat, L., Dignac, M.F., Barré, P., Deldicque, D., Glasser, G.,
Lieberwirth, I., and Chabbi, A.: Nanoscale evidence of contrasted processes for root-derived organic
matter stabilization by mineral interactions depending on soil depth, *Soil Biol. Biochem.*, 85, 82-88,
2015.

550 Schmidt, M.W.I., Torn, M.S., Abiven, S., Dittmar, T., Guggenberger, G., Janssens, I.A., Kleber, M.,
Kögel-Knabner, I., Lehmann, J., Manning, D.A.C., Nannipieri, P., Rasse, D.P., Weiner, S., [and](#)
Trumbore, S.E.: Persistence of soil organic matter as an ecosystem property, *Nature*, 478, 49-56,
2011.

Schumacher, M., Christl, I., Scheinost, A.C., Jacobsen, C., [and](#) Kretzschmar, R.: Chemical
555 heterogeneity of organic soil colloids investigated by scanning transmission X-ray microscopy and
C-1s NEXAFS microspectroscopy, *Environ. Sci. Technol.*, 39, 9094-9100, 2005.

Senn, A.C., Kaegi, R., Hug, S.J., Hering, J.G., Mangold, S., and Voegelin, A.: Composition and
structure of Fe(III)-precipitates formed by Fe(II) oxidation in water at near-neutral pH:
Interdependent effects of phosphate, silicate and Ca, *Geochim. Cosmochim. Acta*, 162, 220--246,
560 2015.

Solomon, D., Lehmann, J., Harden, J., Wang, J., Kinyangi, J., Heymann, K., Karunakaran, C., Lu, Y.,
Wirick, S., and Jacobsen, C.: Micro-and nano-environments of carbon sequestration: Multi-element
STXM-NEXAFS spectromicroscopy assessment of microbial carbon and mineral associations,

Chem. Geol., 329, 53-73, 2012.

565 Torn, M.S., Trumbore, S.E., Chadwick, O.A., Vitousek, P.M., and Hendricks, D.M.: Mineral control of soil organic carbon storage and turnover, *Nature*, 389, 170-173, 1997.

Xiao, J., Wen, Y.L., Li, H., Hao, J.L., Shen, Q.R., Ran, W., Mei, X.L., He, X.H., [and](#) Yu, G.H.: In situ visualisation and characterisation of the capacity of highly reactive minerals to preserve soil organic matter (SOM) in colloids at submicron scale, *Chemosphere*, 138, 225-232, 2015.

570 Vogel, C., Mueller, C.W., Hoschen, C., Buegger, F., Heister, K., Schulz, S., Schloter, M., and Kögel-Knabner, I.: Submicron structures provide preferential spots for carbon and nitrogen sequestration in soils, *Nat. Commun.*, 5, 2947, 2014.

Wen, Y.L., Li, H., Xiao, J., Wang, C., Shen, Q.R., Ran, W., He, X.H., Zhou, Q.S., and Yu, G.H.: Insights into complexation of dissolved organic matter and Al(III) and nanominerals formation in soils under contrasting fertilizations using two-dimensional correlation spectroscopy and high resolution-transmission electron microscopy techniques, *Chemosphere*, 111, 441-449, 2014a.

575

Wen, Y.L., Xiao, J., Li, H., Shen, Q.R., Ran, W., Zhou, Q.S., Yu, G.H., and He, X.H. Long-term fertilization practices alter aluminum fractions and coordinate state in soil colloids, *Soil Sci. Soc. Am. J.*, 78, 2083-2089, 2014b.

580

Wild, B., Schnecker, J., Alves, R.J.E., Barsukov, P., Bárta, J., Čapek, P., Gentsch, N., Gittel, A., Guggenberger, G., Lashchinskiy, N., Mikutta, R., Rusalimova, O., Šantrůčková, H., Shibistova, O., Urich, T., Watzka, M., Zrazhevskaya, G., and Richter, A.: Input of easily available organic C and N stimulates microbial decomposition of soil organic matter in arctic permafrost soil, *Soil Biol.*

Biochem., 75, 143-151, 2014.

585 | Wu, J., Wu, M.J., Li, C.P., [and](#) Yu, G.H.: Long-term fertilization modifies the structures of soil fulvic acids and their binding capability with Al, PloS [One](#), 9, e105567, 2014.

Xu, R.K., Hu, Y.F., Dynes, J.J., Zhao, A.Z., Blyth, R.I.R., Kozak, L.M., and Huang, P.M.: Coordination nature of aluminum (oxy)hydroxides formed under the influence of low molecular weight organic acids and a soil humic acid studied by X-ray absorption spectroscopy, Geochim. Cosmochim. Acta, 590 | 74, 6422-6435, 2010.

Yaron-Marcovich, D., Chen, Y., Nir, S., and Prost, R.: High resolution electron microscopy structural studies of organo-clay nanocomposites, Environ. Sci. Technol., 39, 1231-1238, 2005.

Yu, G.H., Wu, M.J., Wei, G.R., Luo, Y.H., Ran, W., Wang, B.R., Zhang, J.C., and Shen, Q.R.: Binding of organic ligands with Al(III) in dissolved organic matter from soil: implications for soil organic 595 | carbon storage, Environ. Sci. Technol., 46, 6102-6109, 2012.

Zhang, J.C., Zhang, L., Wang, P., Huang, Q.W., Yu, G.H., Li, D.C., Shen, Q.R., and Ran, W.: The role of non-crystalline Fe in the increase of SOC after long-term organic manure application to the red soil of southern China, Europ. J. Soil Sci., 64, 797-804, 2013.

Zhao, X., Zhang R., Xue J. F., Pu C., Zhang X.Q., Liu S. L., Chen F., Lal R., and Zhang H. L.: Chapter 600 | One-Management-Induced Changes to Soil Organic Carbon in China: A Meta-analysis, Adv. Agron., 134, 1-50, 2015.

Zhu, T., Lu, X., Liu, H., Li, J., Zhu, X., Lu, J., and Wang, R.: Quantitative X-ray photoelectron spectroscopy-based depth profiling of bioleached arsenopyrite surface by *Acidithiobacillus*

ferrooxidans, —Geochim. Cosmochim. Acta, 127, 120-139, 2014.

605

Figure Captions

Fig. 1. High-resolution transmission electron microscopy (HRTEM) images of highly reactive minerals ~~from in~~ colloids extracted from ~~the NPKM fertilized~~ soil (Ferralic Cambisol) ~~from three~~ after 24-year long-term (1990-2014) NPKM fertilization ~~treatments~~. (a), TEM images; (b), HRTEM images and selected area electron diffraction (SAED) patterns of the two regions indicated by the blue squares, showing that the black region is a complete crystalline, while the grey region is amorphous; (c-d) energy dispersive X-ray analysis (EDX) images of the region 1 and region 2. ~~Control, no fertilization; NPK, chemical nitrogen, phosphorus and potassium fertilization; NPKM, chemical NPK plus swine manure fertilization.~~ Also see Fig. S2 for similar HRTEM images under the Control and NPK fertilizations.

Fig. 2. Representative NanoSIMS images of $^{12}\text{C}^-$, $^{27}\text{Al}^{16}\text{O}^-$ and $^{56}\text{Fe}^{16}\text{O}^-$ in soil colloids from three contrasting long-term (1990-2014) fertilization treatments (Control, no fertilization, $28 \times 28 \mu\text{m}^2$; NPK, chemical nitrogen, phosphorus and potassium fertilization, $30 \times 30 \mu\text{m}^2$; NPKM, chemical NPK plus swine manure fertilization, $25 \times 25 \mu\text{m}^2$). Note that the color intensity calibration bar displayed in the chemical maps corresponds to the relative concentrations of individual elements, but cannot be used to compare one element with another. Bar = $5 \mu\text{m}$.

Fig. 3. Box plots of $^{12}\text{C}^-/^{27}\text{Al}^{16}\text{O}^-$ (a, b) and $^{12}\text{C}^-/^{56}\text{Fe}^{16}\text{O}^-$ (c, d) ratios reflecting the $^{12}\text{C}^-$ rich ROIs (a, c) and $^{12}\text{C}^-$ less rich ROIs (b, d) of the soil colloids from three contrasting long-term (1990-2014) fertilization treatments using NanoSIMS (for all spots). Control, no fertilization; NPK, chemical nitrogen, phosphorus and potassium fertilization; NPKM, chemical NPK plus swine manure fertilization.

The ^{12}C -rich ROIs include the areas above 90 pixels and the ^{12}C -less rich ROIs include the areas in the range of 90-40 pixels under Control and NPK, which were above 50 pixels and in the range of 50-30 pixels under NPKM. The number n in figures represents the number of the selected ROIs. The line in the middle of the box is the median value and the square in the box is the mean value. The lines that protrude out of the boxes represent the 25th and 75th population percentiles. Outliers are shown as diamonds.

Fig. 4. XPS peak-fitting (Al $2p_{3/2}$ and C 1s) images recorded from soil (Ferralic Cambisol) colloids extracted under three long-term (1990-2014) fertilization treatments. Control, no fertilization; NPK, chemical nitrogen, phosphorus and potassium fertilization; NPKM, chemical NPK plus swine manure fertilization.

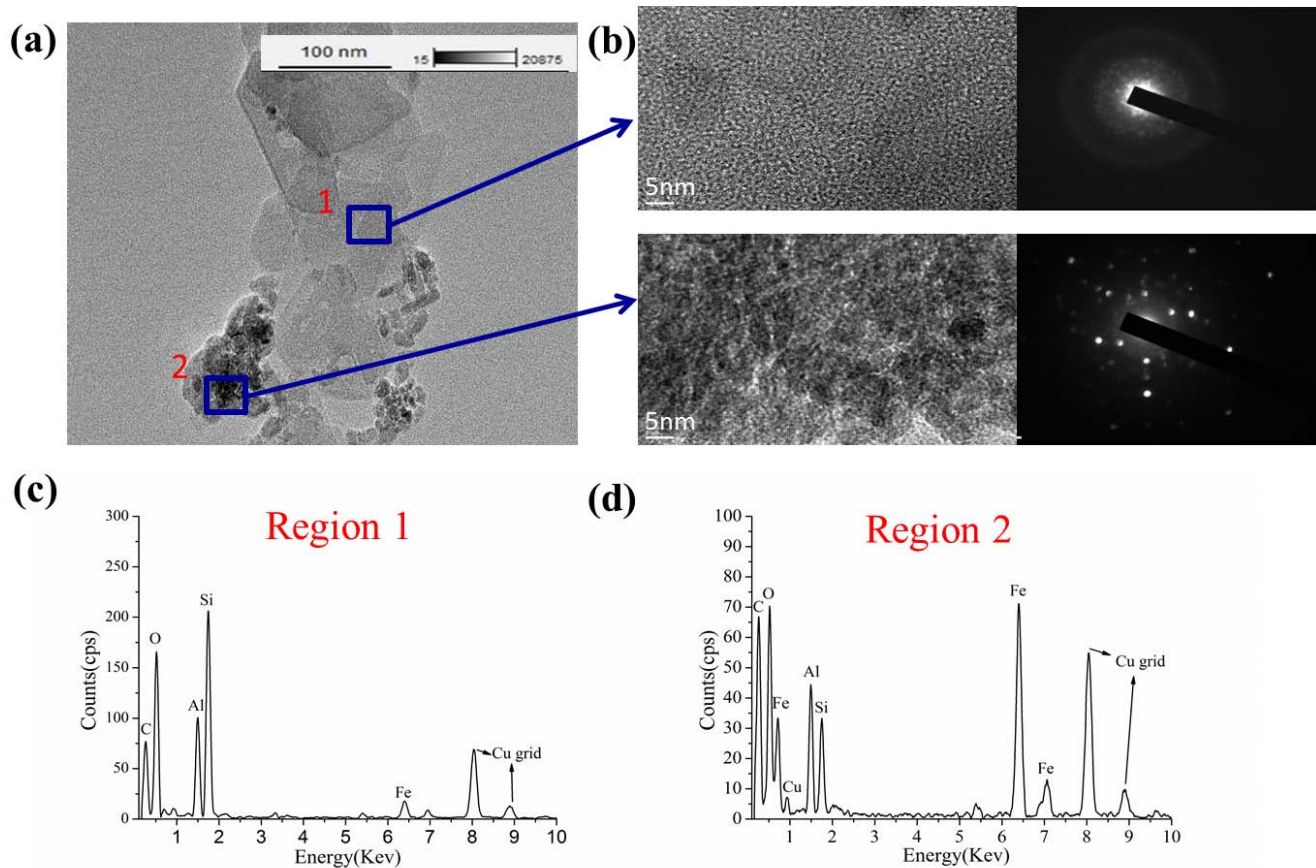
Fig. 5. Fe K-edge EXAFS (left) and Fourier transforms (right) of reference materials and soil colloids from three contrasting long-term (1990-2014) fertilization treatments. Control, no fertilization; NPK, chemical nitrogen, phosphorus and potassium fertilization; NPKM, chemical NPK plus swine manure fertilization.

640 **Table Captions**

Table 1. Basic physiochemical characteristics of soil samples from three contrasting long-term (1990-2014) fertilization treatments ^a.

Table 2. Binding energy and quantitation/assignment of XPS spectral bands of soil samples from three contrasting long-term (1990-2014) fertilization treatments ^a.

645 **Table 3.** Linear combination fit (LCF) results of Fe K-edge XANES spectra of the soil colloids from three contrasting long-term (1990-2014) fertilization treatments ^a.



650 **Figure 1**

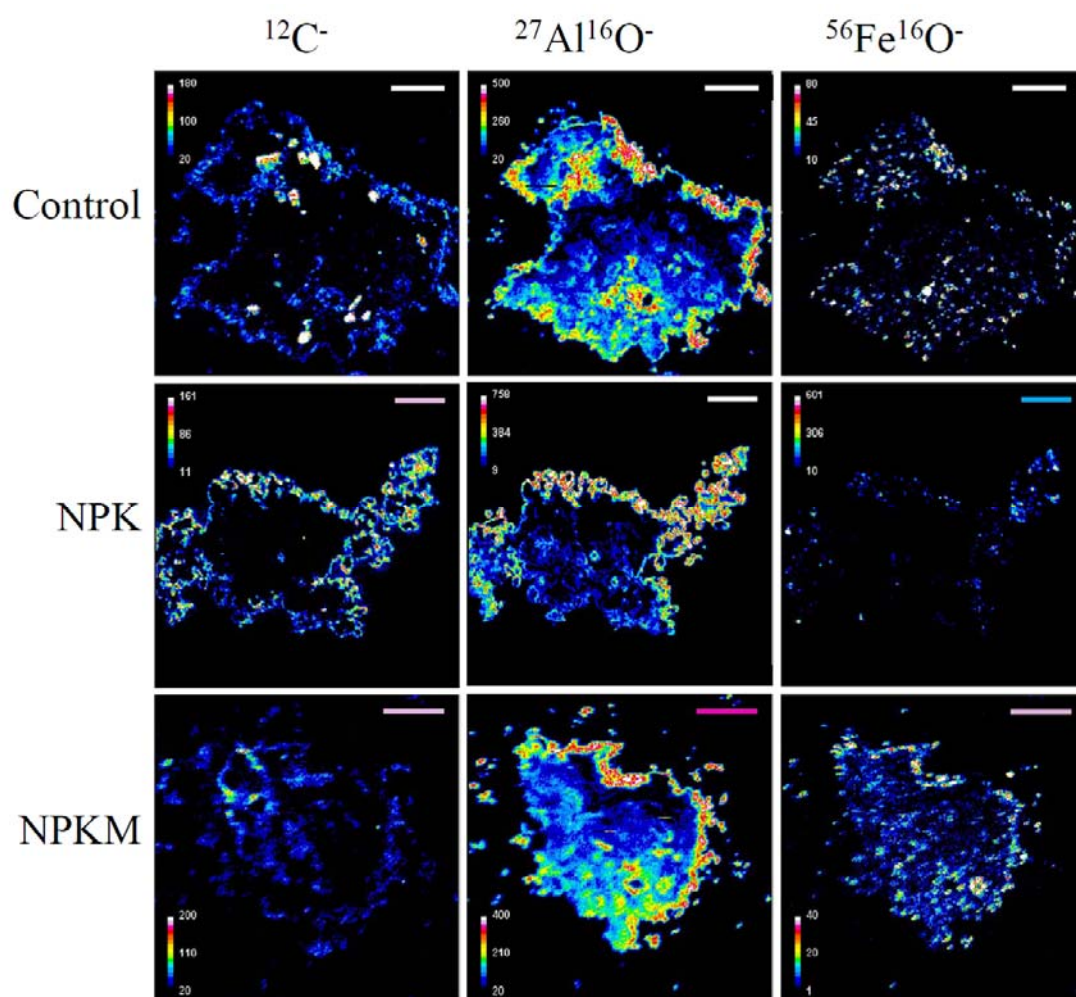
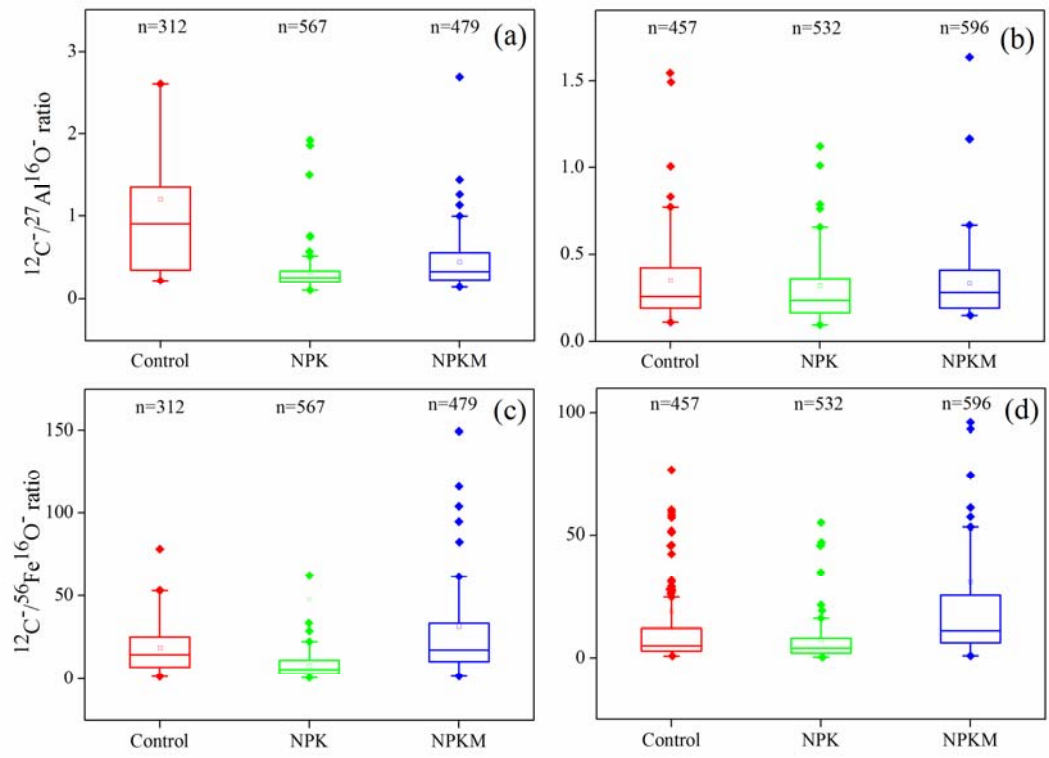


Figure 2



655 **Figure 3**

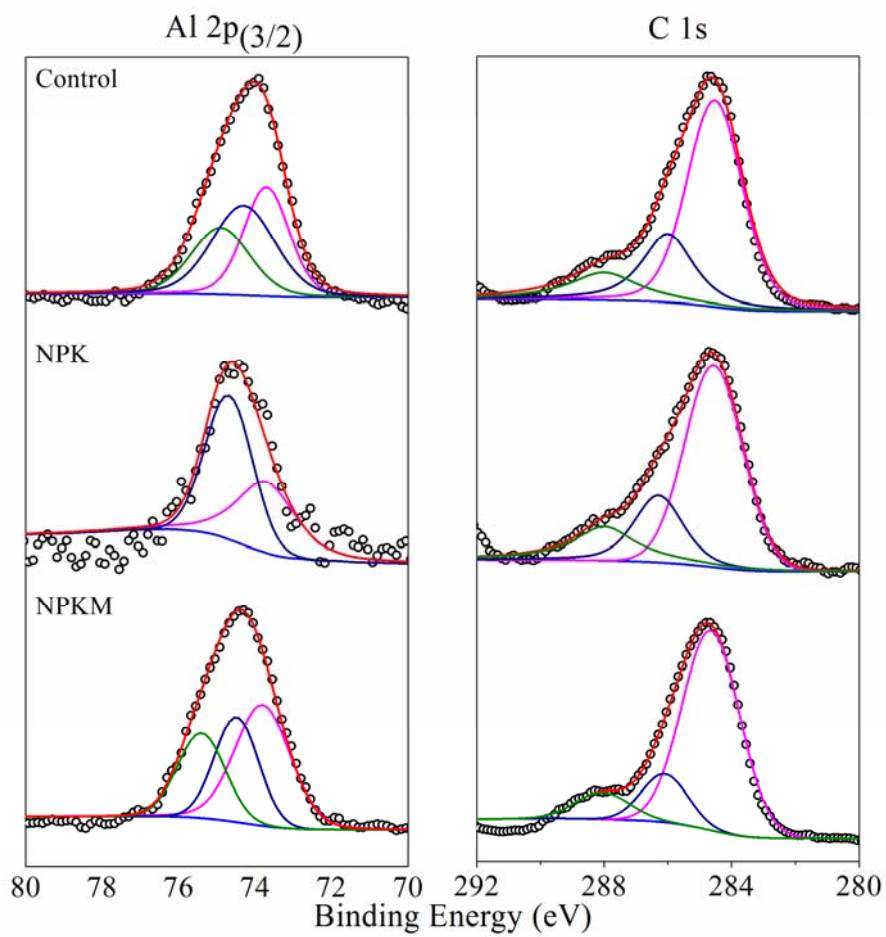
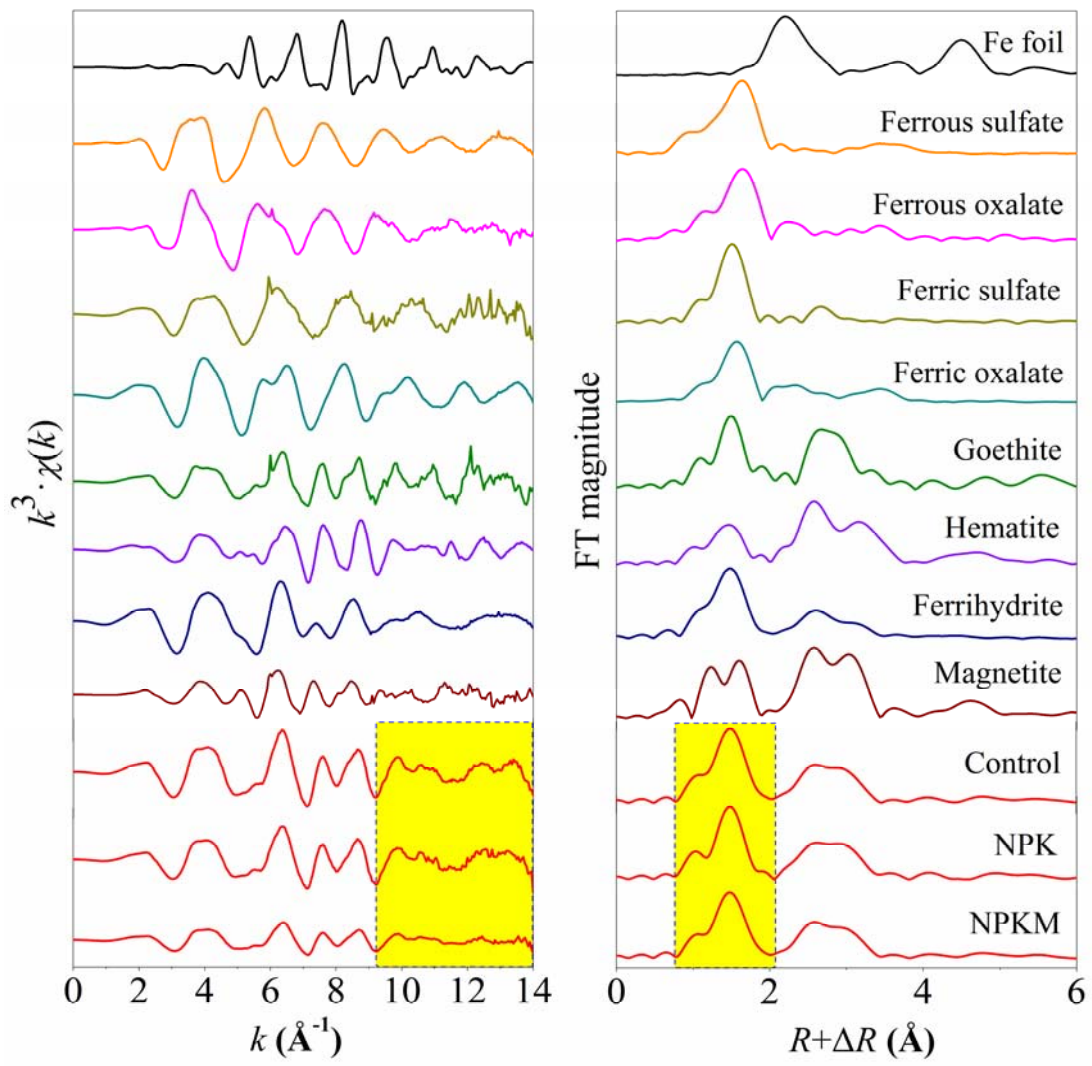


Figure 4



660 **Figure 5**

Table 1. Basic physiochemical characteristics of soil samples from three separate long-term (1990-2014) fertilization treatments ^a.

Treatment	Soil					Soil colloids				
	Bulk soil pH (H ₂ O)	SOM (g kg ⁻¹)	Al _o (%)	Fe _o (%)	SRO (%)	Al _{XPS} (%)	Fe _{XPS} (%)	DOC (mg L ⁻¹)	DOC/Al _{XPS}	DOC/Fe _{XPS}
Control	5.47 ± 0.04b	14.88 ± 2.02c	0.07 ± 0.003b	0.20 ± 0.004b	0.17 ± 0.00b	6.23	1.47	6.17	0.99	4.20
NPK	4.15 ± 0.00c	18.36 ± 0.16b	0.04 ± 0.003c	0.16 ± 0.003c	0.12 ± 0.00c	1.22	0.48	4.62	3.79	9.63
NPKM	5.84 ± 0.01a	25.13 ± 2.02a	0.11 ± 0.002a	0.30 ± 0.007a	0.26 ± 0.01a	6.84	1.59	42.02	6.14	26.43

^aNote: Control, no fertilization; NPK, chemical nitrogen, phosphorus and potassium fertilization; NPKM, chemical NPK plus swine manure fertilization, SOM, soil organic matter. Al_{XPS} and Fe_{XPS} indicated the surface concentration of Al and Fe in soil colloids, which were determined by the X-ray photoelectron spectroscopy (XPS). Al_o and Fe_o indicated reactive Al and Fe nanominerals, which were extracted using acid ammonium oxalate. DOC, dissolved organic carbon in soil colloids. Short-range ordered (SRO) minerals were calculated using the formula of Al_o + 1/2 Fe_o (%) (Kramer et al., 2012). Significant differences among fertilization treatments were determined using one-way ANOVA followed by the Tukey's HSD post hoc test at $P < 0.05$ after the conditions of normality and homogeneity of variance were met.

Table 2. Binding energy and quantitation/assignment of XPS spectral bands of soil samples from three separate long-term (1990-2014) fertilization treatments ^a.

Element	Control			NPK			NPKM		
	Peak (eV)	Atomic (%)	Assignment	Peak (eV)	Atomic (%)	Assignment	Peak (eV)	Atomic (%)	Assignment
Al 2p _{3/2}	73.8	34.2	Allophane Al ₂ O ₃ / Al ₂ O ₃ -nH ₂ O	73.8	42.9	Allophane Al ₂ O ₃ / Al ₂ O ₃ -nH ₂ O	73.8	45.1	Allophane Al ₂ O ₃ / Al ₂ O ₃ -nH ₂ O
Al 2p _{3/2}	74.3	39.0	Boehmite AlO(OH)	74.7	57.1	Boehmite AlO(OH)	74.5	29.4	Boehmite AlO(OH)
Al 2p _{3/2}	74.9	26.8	AlOx	/	/	/	75.4	25.5	AlOx
C 1s	284.6	62.3	Aromatic carbon (Ar-C-C/Ar-C-H)	284.6	62.5	aromatic carbon (Ar-C-C/Ar-C-H)	284.6	75.9	aromatic carbon (Ar-C-C/Ar-C-H)
C 1s	286.1	23.6	Ether or alcohol carbon (C-O)	286.2	20.8	Ether or alcohol carbon (C-O)	286.1	14.7	Ether or alcohol carbon (C-O)
C 1s	288.0	14.2	Ketonic or aldehyde carbon (C=O)	288.0	16.7	Ketonic or aldehyde carbon (C=O)	288.0	9.5	Ketonic or aldehyde carbon (C=O)

^aNote: Control, no fertilization; NPK, chemical nitrogen, phosphorus and potassium fertilization; NPKM, chemical NPK plus swine manure fertilization. The atomic percentage (%) is the corrected value calculated from the XPS peak-fitting areas (Childs et al., 1997; Crist, 2000) and elemental assignments were determined from published studies (Liang et al., 2008; Mikutta et al., 2009; Xiao et al., 2015).

675 **Table 3. Linear combination fit (LCF) results of Fe K-edge XANES spectra of the soil colloids from three separate long-term (1990-2014) fertilization treatments ^a.**

Treatment	LCF results (%)						LCF parameters	
	Goethite	Hematite	Ferrihydrite	Ferric sulfates	Ferrous citrates	Ferrous sulfates	R-factor	Chi-square
Control	66.0 ± 0.025	14.9 ± 0.000	16.0 ± 0.025	ND	3.10 ± 0.012	ND	0.000052	0.00437
NPK	67.0 ± 0.025	25.0 ± 0.000	6.30 ± 0.020	ND	ND	1.70 ± 0.008	0.000051	0.00426
NPKM	56.8 ± 0.025	20.4 ± 0.000	18.0 ± 0.017	4.8 ± 0.018	ND	ND	0.000051	0.00436

^a Note: Control, no fertilization; NPK, chemical nitrogen, phosphorus and potassium fertilization; NPKM, chemical NPK plus swine manure fertilization. ND, not detected. Determination of parameters of fit (i.e., R-factor and chi-square) indicated that the LCF results are convincing.